Ashesi Solar Monitoring Network (ASMONET): An IoT-Enabled Network for Ground-Based Soiling Measurements in West Africa

Francis Aweenagua[1], Stewart Isaacs[2], Jeremiah Takyi[1] and Heather R. Beem[1]

[1]Department of Engineering, Ashesi University, Berekuso, Eastern Region, Ghana
[2]Department of Aeronautics and Astronautics, Massachusetts Institute of Technology, Cambridge, MA, USA

***Abstract* — Photovoltaic energy generation has grown substantially in West Africa within the past few years. Dust soiling, however, can reduce generation capacity, especially during the dry season (Harmattan) in this context. Soiling impacts are ideally assessed using ground-based measurements; however, such systems are sparse or missing entirely in the region, leaving gaps in understanding the true extent of soiling impact locally. This work aims to improve solar data availability in West Africa through the design of a ground-based, IoT-enabled PV sensor system to be installed throughout the region, forming a network. The system leverages a two-panel, one-coupon experimental approach to measuring soiling mass accumulation and a sensor suite to provide real-time and historical data on panel performance, air quality, and weather conditions, among others. Preliminary tests show reliable collection of ground-based data and transmission to the cloud for remote access and analysis, highlighting the system's potential as a research platform for analysis and insight generation on solar PV in West Africa.**

I. Introduction

Photovoltaic (PV) energy generation is increasing as the world moves to decarbonize its sources of electricity. In 2023, nearly 350 GW of PV capacity was installed, and by 2030, the number is expected to reach nearly 500 GW [1]. However, solar panels are impacted by environmental factors, such as dust soiling - a phenomenon that occurs when dust and other particles settle on the surface of a panel, obscuring incoming light and reducing power output [2], [3]. The recent increase in solar usage, particularly in dry desert climates, has led to a boon in research interest in dust-soiling effects on PV systems. These studies have produced estimates that soiling could have cost $7Bn annually in lost revenues in 2023 [4],[5].

PV systems are also being explored as a method to increase energy access and advance the United Nation's Sustainable Development Goal 7, which aims to secure universal access to modern energy [6]. This is especially true in rural areas of Africa, where energy access is lagging [6]. Since many West African countries have large rural populations, there is potential for a considerable amount of solar to be installed in the region. However, the region can experience significant soiling loss when the annual dry season (Harmattan) brings in dry dust-laden air from the nearby Sahara Desert [7]. In the worst locations, PV systems may lose more than 50% of power output to dust-soiling [7].

Soiling impacts are most accurately assessed via ground-based measurements. However, existing measurements for air quality and solar panels under soiling are sparse across the African continent. For example, in a global soiling loss study involving 132 ground-based solar installation sites, only three of the sites were located within West Africa, all of which were in Nigeria [8]. This leaves a gap in understanding the true extent of soiling and its impacts on achieving energy access goals in the West African region.

This work aims to improve solar data availability in West Africa by designing a network of ground-based, IoT-enabled PV sensor systems to be installed throughout the region. Each system will provide data on solar panel performance, key environmental parameters affecting dust soiling, soiling mass accumulation, and relative loss in power output. Once in place, this network will give researchers insight into regional solar panel performance and the reduction effects of environmental conditions such as air pollution and Harmattan. The collected data can be used to advance energy access goals by improving solar PV performance and models for soiling loss and, ultimately, aid in the design of reliable PV systems.

II. Methods

A. System Architecture

There are three fundamental sub-systems of the Ashesi Solar Monitoring Network (ASMONET): a weather station, a PV module soiling monitoring system, and a cloud-based web application. The first two, e.g., the hardware, are shown in Fig. 1. The weather station provides data on the relative humidity, ambient temperature, wind speed and direction, particulate matter concentration, and the amount of rainfall. The PV module soiling monitoring system contains several components. Soiling is measured in terms of the mass of dust, and this is captured through a three-part setup comprising a control module, a test PV module, and a complementary glass coupon. A weighing scale is used to measure the cumulative mass of the soiled coupon. An irradiance sensor is integrated into the system to measure the solar irradiance at the monitoring site. The performance of the PV modules is measured using power sensors connected to each panel and integrated into a data acquisition system. Solar power equipment, including charge controllers, inverters, batteries,

and loads, are incorporated into the system to form a complete solar power system. An MPPT charge controller is deployed in the system to regulate the charging of a 147Ah lead acid battery in each PV module setup. Each battery is also connected to an inverter to power AC components, including an irradiance data acquisition device, a Wi-Fi router, and an auxiliary load (a 10W flood light) controlled by a relay switch. Data from the system is sampled at a sampling rate of every three (3) minutes and uploaded to the cloud for storage and analysis. The final sub-system, a cloud-based web application, is seamlessly integrated to allow for remote access to the data and enable users to perform quick analysis and visualization.

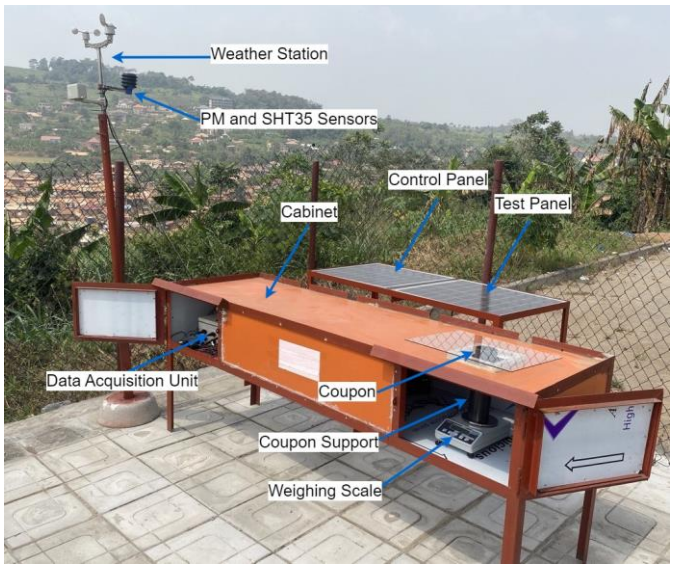

Fig. 1. The data collection component of ASMONET showing some of the system's major parts.

B. Environmental Data

PV module soiling and performance are known to be affected by environmental conditions such as ambient temperature, relative humidity, wind speed and direction, and rainfall [9], [10]. Indeed, several studies have focused on understanding the impact of weather and environmental conditions on PV module performance [9]-[13], indicating the relevance of collecting such data for PV research purposes. These environmental conditions exhibit both spatial and temporal variations; hence, including their ground-based measurements will enable a more effective interpretation of panel performance at the experiment site. Additionally, given that ground-based environmental data like particulate matter concentration, relative humidity, and ambient temperature are sparsely available across West Africa, this platform can serve as a data source for other research purposes such as air pollution and climate change studies.

ASMONET presents a solution to the problem of ground weather and environmental data availability in West Africa for research purposes. ASMONET uses Argent Data Systems' Weather Sensor Assembly p/n 80422 to measure the amount of rainfall, wind speed, and wind direction. A SEN54 particulate matter sensor is integrated into the weather station to measure the concentrations of PM1.0, PM2.5, PM4, and PM10 particle size ranges. In addition, an SHT35 sensor is deployed to collect relative humidity and ambient temperature data. The weather station is mounted on a stand to be positioned about 1900mm above the ground, allowing unimpeded access to rain and wind flow.

TABLE I
PV MODULE ELECTRICAL CHARACTERISTICS AND SPECIFICATIONS.

Electrical Specification at STC	Value
Maximum Power (P_{max})	100W
Open-Circuit Voltage (V_{oc})	23.3V
Voltage At P_{max} (V_{mp})	19.8V
Short-Circuit Current (I_{sc})	5.45A
Current At P_{max} (I_{mp})	5.05A
Cells Efficiency (%)	22.42%
Power Temperature Coefficient	-0.43%/℃
Voltage Temperature Coefficient	-0.34%/℃
Current Temperature Coefficient	0.05%/℃

C. PV Module Performance

ASMONET uses two SGM-100W PV modules for PV performance measurement and soiling estimation. Both panels are ground-mounted with a tilt angle of ≈3º facing the north-west cardinal direction. Both monocrystalline PV modules at Standard Test Condition (STC) have a rated peak power of 100W, open-circuit voltage (V_{oc}) of 23.3V and a short-circuit current (I_{sc}) of 5.45A. Table I outlines the electrical specifications of the PV module used by ASMONET.

The Global Horizontal Irradiance (GHI) at the experiment site is measured using a Vernier LabQuest 2 Data Logger with an upward-facing and horizontally oriented pyranometer. Irradiance data is recorded and stored on the data logger with a time resolution of 3 minutes, and it is uploaded to the cloud database once a week through the ASMONET web application.

PV module performance is measured using INA226 power sensors connected to each PV module. The power sensor measures the panel current, voltage, and power during operation. In addition, the PV module temperature is measured with a DS18B20 temperature sensor cased in a flat-surfaced stainless steel square probe. A temperature sensor is attached to the back of a PV cell of each PV module using copper foil tape. Fig. 2 shows how the temperature sensor was attached to the PV module. This mounting approach was chosen to conform to the IEC standards stipulated in [14]. The measured

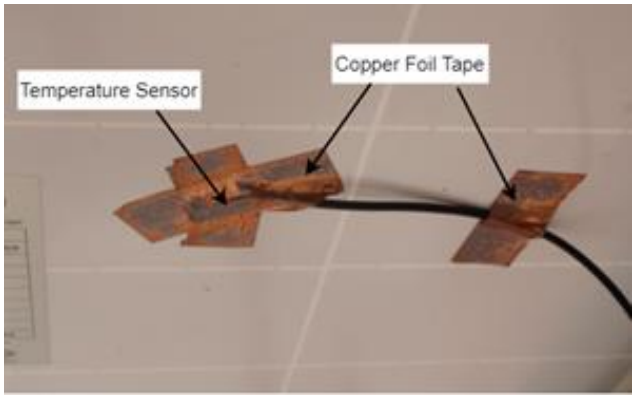

Fig. 2. PV module temperature measurement using DS18B20 temperature sensor and copper foil tape.

performance parameters are used to determine the performance ratio (PR) of each PV module using (1) [14], where τ_k represents the sampling time, $P_{out,k}$ represents the power output of the panel, P_0 represents the PV module power rating at STC, $G_{i,k}$ represents the measured irradiance and $G_{i,ref}$ represents the irradiance at STC [14]. Additionally, the PV modules' temperature-corrected performance ratios ($PR'_{25℃}$) are calculated using the 25^0C performance ratio in (2), where $C_{k,25℃}$ is a power rating temperature adjustment factor calculated using (3), where $T_{mod,k}$ represents the measured PV module temperature and γ is the relative maximum-power temperature coefficient of the PV module [14]. Both PR and $PR'_{25℃}$ are computed at 6:00 pm each day using data recorded seven days prior to the day of computation. Therefore, the performance ratio data from ASMONET is not computed in real-time but is delayed by seven days.

$$PR = \left(\sum_k P_{out,k} \times \tau_k\right) \Big/ \left(\sum_k \frac{P_0 \times G_{i,k} \times \tau_k}{G_{i,ref}}\right) \quad (1)$$

$$PR'_{25℃} = \left(\sum_k P_{out,k} \times \tau_k\right) \Big/ \left(\sum_k \frac{(C_{k,25℃} \times P_0) \times G_{i,k} \times \tau_k}{G_{i,ref}}\right) \quad (2)$$

$$C_{k,25℃} = 1 + \gamma \times (T_{mod,k} - 25℃) \quad (3)$$

D. Soiling Measurement

ASMONET aims to be a robust platform for estimating PV module soiling at any given location. This is done through an experimental design involving two identical PV modules and one coupon. One PV module is marked as the control panel, while the other is labeled as the test panel. The control panel is wet cleaned with a clean paper towel at least twice a week, while the test panel is allowed to soil naturally. Both panels are mounted in close proximity to each other to ensure both experience the same solar irradiance. The coupon is also mounted adjacent to the test panel and allowed to soil naturally with the test panel. The coupon is made of transparent 3mm float glass with dimensions 500mm by 400mm. It acts as a soiling collection surface for mass measurement. Fig. 3 illustrates the PV soiling measurement architecture employed by ASMONET.

Twice every week, the mass of dust on the coupon is determined by weighing the coupon with the accumulated dust particles and subtracting the known mass of the clean coupon. During each measurement process, the mass measurement is repeated about seven times, and each mass value is recorded through the ASMONET web application. An average of the seven sample readings is computed for further visualization and analysis. ASMONET's dust mass measurement is premised on two primary assumptions: first, that dust particles are randomly distributed and move randomly under normal atmospheric conditions, and second, that the random distribution of dust particles results in the equal soiling of surfaces of the same surface area at the same location.

Based on these salient assumptions, the mass of dust accumulation on the test PV module is estimated using (4),

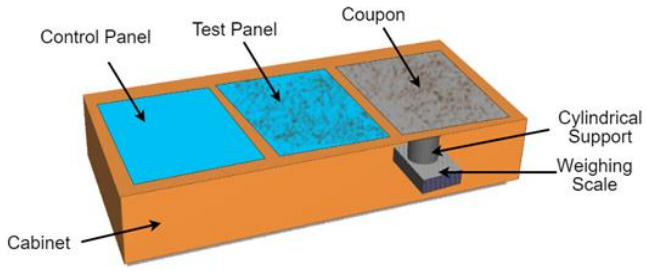

Fig. 3. Soiling measurement experimental architecture using two panels and a glass coupon.

where m_p and m_c represent the mass of dust deposited on the panel and coupon, respectively, and A_p and A_c represents the surface areas of the panel and coupon, respectively.

$$m_p = \frac{A_p \times m_c}{A_c} \quad (4)$$

PV module soiling-related losses are estimated using the soiling ratio (r_s) and soiling loss (r_{loss}) calculated at 6 pm daily using data collected between 6 am and 6 pm. Both soiling matrices are calculated using (5) and (6), respectively, where Z_{soil} represents the performance output of the soiled panel (test panel) and Z_{clean} represents the performance output of the clean panel (control panel). The PV module's maximum power output (P_{max}) is used to compute both soiling matrices since it has been found to provide better results as compared to using

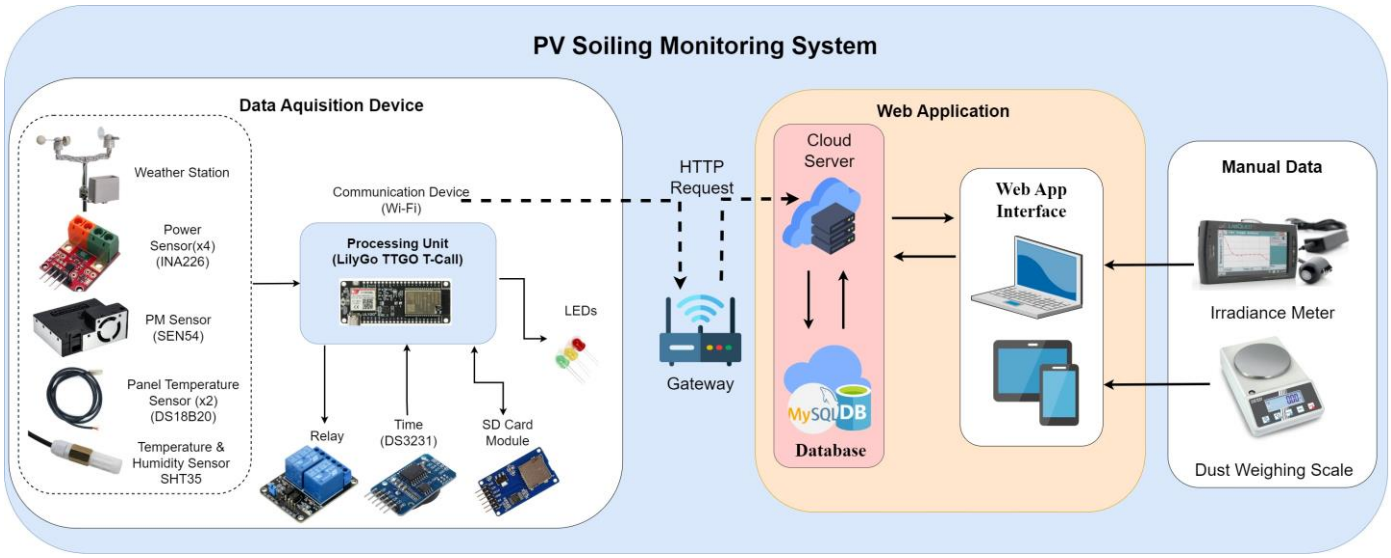

Fig. 4. The IoT architecture of the monitoring system showing data flow from the sensors to the cloud.

the short-circuit current (I_{sc}), especially in cases of nonuniform soiling [15], [16]. The soiling matrices are stored in the database once computed and displayed on the web application dashboard for visualization and analysis.

$$r_s = \frac{Z_{soil}}{Z_{clean}} \tag{5}$$

$$r_{Sloss} = |1 - r_s| \tag{6}$$

E. Web Application Interface

Once all measured and derived data are obtained by the system, they are stored in a cloud-based database for subsequent analysis and generation of insight. The data from the data acquisition system is transmitted to the cloud via HTTP request through a Wi-Fi communication network. The data is stored in a structured relational database on the cloud with tables for the diverse data requiring cloud storage. A responsive web application hosted in the cloud is also developed and seamlessly integrated to facilitate remote user interaction with the data. Fig. 4 illustrates the IoT system architecture that manages real-time data acquisition, storage, and interaction.

Two forms of data storage are implemented for ASMONET: a cloud-based data storage and an SD card-based local data storage. The cloud-based data storage system allows for remote access to the data for analysis and real-time system monitoring. On the other hand, the SD card-based local storage serves two primary functions: 1. provide a local backup storage option for the cloud data and 2. provide temporal storage for data that failed to be transmitted to the cloud due to network interruptions. This data is retrieved and retransmitted once the internet connection is restored after any interruptions.

Data from the database is fetched and displayed on the web application dashboard using diverse visualization techniques to facilitate quick analysis. The web application dashboard displays the current and last ten environmental condition recordings, including the ambient temperature, relative humidity, amount of rainfall, wind speed, PM 2.0, and PM 10.0 concentrations, among other conditions, in real-time. This provides a synopsis of the current weather conditions at the data collection site for real-time insight generation. Also, the dashboard displays the performance output (current, voltage, power) and temperature of both control and test PV modules in real-time. These parameters are displayed side by side for a quick comparative analysis of the state and performance of both PV modules. Fig 5. shows a snapshot of the web application dashboard interface. The ASMONET web application dashboard also displays visualizations of the daily

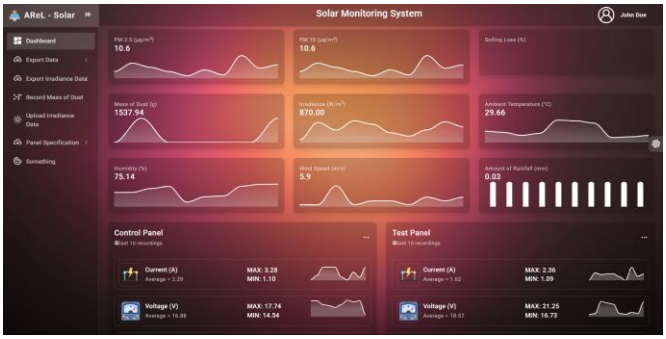

Fig. 5. ASMONET web application dashboard showing visualizations of real-time data from the monitoring system.

total energy generated by both PV models, the hourly average panel current, the hourly average panel power, the hourly average charging current, and the hourly average battery voltage. The PV modules' daily soiling ratio, performance ratio, and temperature-corrected performance ratios are also graphically illustrated on the dashboard for ready analysis of the PV module performance on the go.

The ASMONET web application enables users to perform other functionalities, including manually recording the mass of dust on the coupon through an input form and manually uploading the irradiance data by uploading a CSV file obtained from the LabQuest data logger. The web application parses the CSV file, extracts the irradiance data, and stores it in the database with the corresponding timestamp for each data point. A user can export any recorded data in a CSV file format to conduct further comprehensive and complex data analysis using external data analysis tools. The system also makes available the specifications of the PV modules in Excel, PDF, and web page formats for easy access to all information on the PV modules.

III. Results

Data was collected from December 2023 to May 2024, exported from the web application, and processed. In a few cases, ASMONET was offline due to repairs, in which case a forward-filling algorithm was used to fill in missing data from these times. A sampling of the results of environmental and power generation data is presented here.

A. Environmental Data

PM concentration data in micrograms per meter cubed is given in Fig. 6. PM concentration values for particles with aerodynamic diameters less than 1, 2.5, and 10 micrometers are given in blue, orange, and green, respectively. The gray band indicates dates during the annual Harmattan season, from November to March. During the Harmattan season, when there is less precipitation and an influx of dust from the Sahara Desert in the region, PM concentrations for all sizes increase as expected. Values peak above 300 micrograms per meter cubed in February, with slightly higher concentrations for PM10 since dust particles tend to have larger diameters. However, PM concentrations remain relatively lower after the Harmattan season, with slightly more precipitation and fewer atmospheric dust particles.

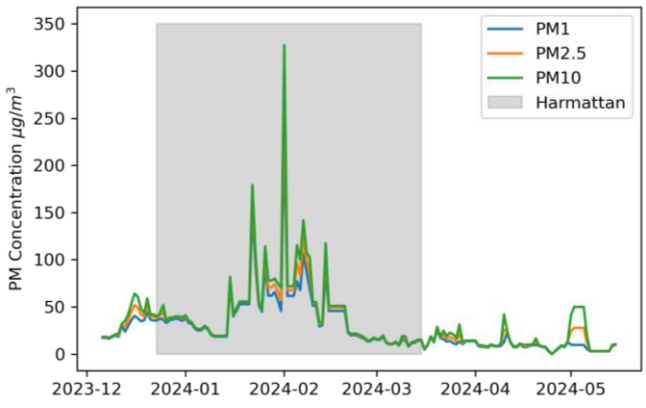

Fig. 6. PM concentration from December 2023 to May 2024 showing the effects of Harmattan on PM concentration.

Recorded wind speeds and direction are presented in a wind rose, shown in Fig. 7. Wind speed data was filtered to account for outlier values more than two standard deviations greater than the average. Each bar corresponds to the direction of the recorded wind, with the height of the bar indicating frequency (longer bars indicate greater frequency in a given direction). The colors correspond to the wind speed, with darker colors corresponding to faster wind speeds. During this time, wind primarily originated from the West and Southwest directions.

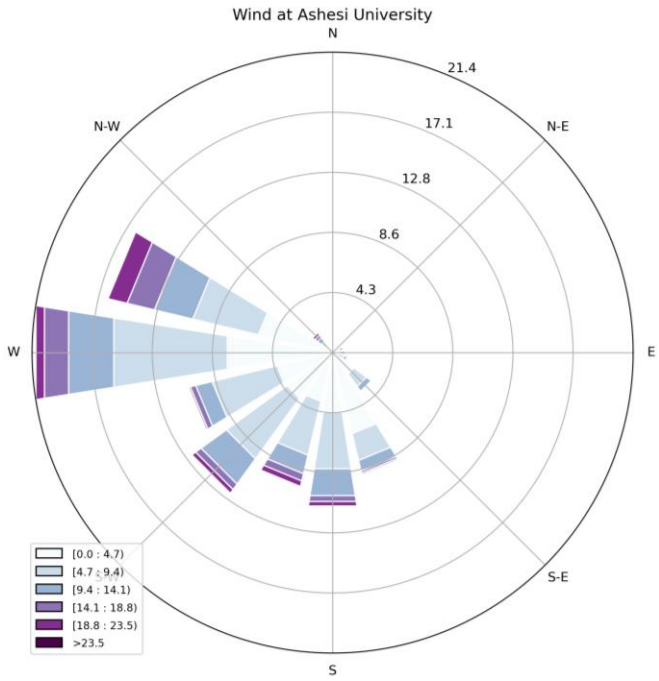

Fig. 7. Wind rose showing the wind direction and the corresponding speed from December 2023 to May 2024

The fastest wind speeds came from the Northwest, with speeds as high as 20 m/s in some measurements.

B. PV Performance

Fig. 8. shows the irradiance measurements and the performance of one of the PV modules on January 25, 2024. The maximum available irradiance measured in watts per square meter [W/m2] at the data collection site was measured to be just above 700 W/m2. This peak irradiance was observed

around 1:00 pm. During that same time, the maximum power output from the panel for that day was recorded to be around 57W. It is also evident from Fig. 8. that there is a very close association between the measured solar irradiance and the output of the PV module, which is highly expected. Also, frequent shading from clouds on the day can be seen to have impacted the performance of the panel. This can be observed by the frequent drop in power output characterized by a similar drop in the available irradiance measured.

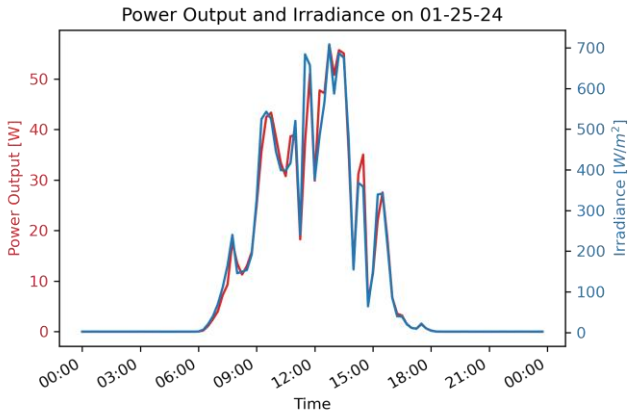

Fig. 8. Irradiance and power output of PV module on January 25, 2024

.

IV. Discussion

A first-of-its-kind ground-based and IoT-enabled solar monitoring system has been designed and installed. Several considerations informed the design of the system architecture, identification of relevant parameters to measure, selection of appropriate sensors, forming a reliable and relevant platform for solar PV research in the West African region. The experimental design for soiling measurements allows for a comparative approach, and the custom-built web application is versatile across the presentation of real-time data and exporting of past data. The system is operational and has shown its capability of capturing PV power generation, solar irradiance, particulate matter concentration, and other relevant environmental data, made available for download via an online web-app interface. A sampling of preliminary results confirms sensor readings within expected ranges, especially across seasonal changes.

Once several more months of time-series data are available, further analysis will be conducted. For example, power generation and dust mass measurements will be compared to existing soiling models that estimate deposition and power reductions. This will enable evaluation of the models' accuracy within the region and offer improvements, if necessary. ASMONET's ground-based measurements will be compared with data derived from other sources for the region so as to identify any key areas of differentiation worth drawing attention to. Particulate matter concentration measurements can also be shared with air quality researchers in Africa to study the impact of dust and other aerosols on human health.

Future work includes refining the quality of the incoming data across the remaining parameters and working with other institutions in the area to replicate this system, thus building the network.

References

[1] "World Energy Outlook 2023," International Energy Agency (IEA), 2023. [Online]. Available: https://www.iea.org/reports/world-energy-outlook-2023

[2] A. Sayyah, M. N. Horenstein, and M. K. Mazumder, "Energy yield loss caused by dust deposition on photovoltaic panels," *Solar Energy*, vol. 107, pp. 576–604, Sep. 2014, doi: 10.1016/j.solener.2014.05.030.

[3] T. Sarver, A. Al-Qaraghuli, and L. L. Kazmerski, "A comprehensive review of the impact of dust on the use of solar energy: History, investigations, results, literature, and mitigation approaches," *Renewable and Sustainable Energy Reviews*, vol. 22, pp. 698–733, Jun. 2013, doi: 10.1016/j.rser.2012.12.065.

[4] B. Aïssa *et al.*, "A Comprehensive Review of a Decade of Field PV Soiling Assessment in QEERI's Outdoor Test Facility in Qatar: Learned Lessons and Recommendations," *Energies*, vol. 16, no. 13, Art. no. 13, Jan. 2023, doi: 10.3390/en16135224.

[5] K. Ilse *et al.*, "Techno-Economic Assessment of Soiling Losses and Mitigation Strategies for Solar Power Generation," *Joule*, vol. 3, no. 10, pp. 2303–2321, Oct. 2019, doi: 10.1016/j.joule.2019.08.019.

[6] "Africa Energy Outlook 2022," IEA, Paris, 2022. [Online]. Available: https://www.iea.org/reports/africa-energy-outlook-2022

[7] S. Isaacs *et al.*, "Dust soiling effects on decentralized solar in West Africa," *Applied Energy*, 2023, [Online]. Available: https://doi.org/10.1016/j.apenergy.2023.120993

[8] Md. M. H. Mithhu, T. A. Rima, and M. R. Khan, "Global analysis of optimal cleaning cycle and profit of soiling affected solar panels," *Applied Energy*, vol. 285, p. 116436, Mar. 2021, doi: 10.1016/j.apenergy.2021.116436.

[9] V. Gupta, M. Sharma, R. K. Pachauri, and K. N. D. Babu, "Comprehensive review on effect of dust on solar photovoltaic system and mitigation techniques," *Solar Energy*, vol. 191, pp. 596–622, 2019, doi: https://doi.org/10.1016/j.solener.2019.08.079.

[10] I. S. Al Jassasi *et al.*, "Experimental investigation of the soiling effect on the PV systems performance and the cleaning intervals in Oman," *Solar Energy Advances*, vol. 3, p. 100045, Jan. 2023, doi: 10.1016/j.seja.2023.100045.

[11] C. D. Pero, N. Aste, and F. Leonforte, "The effect of rain on photovoltaic systems," *Renewable Energy*, vol. 179, pp. 1803–1814, 2021, doi: https://doi.org/10.1016/j.renene.2021.07.130.

[12] C. Schwingshackl *et al.*, "Wind Effect on PV Module Temperature: Analysis of Different Techniques for an Accurate Estimation," *Energy Procedia*, vol. 40, pp. 77–86, 2013, doi: https://doi.org/10.1016/j.egypro.2013.08.010.

[13] A. Vasel and F. Iakovidis, "The effect of wind direction on the performance of solar PV plants," *Energy Conversion and Management*, vol. 153, pp. 455–461, 2017, doi: https://doi.org/10.1016/j.enconman.2017.09.077.

[14] I. Standard and others, “IEC 61724-1 Photovoltaic System Performance—Part 1: Monitoring,” *NSAI Standard*, 2021.
[15] D. Braga *et al.*, “Uniform and non-uniform soiling of PV modules: A comprehensive study of performance and temperature effects,” in *Proceedings 45th IEEE Photovoltaic Specialists Conference and the WCPEC-7, Hawaii*, 2018.
[16] M. Gostein, T. Düster, and C. Thuman, “Accurately measuring PV soiling losses with soiling station employing module power measurements,” in *2015 IEEE 42nd Photovoltaic Specialist Conference (PVSC)*, 2015, pp. 1–4. doi: 10.1109/PVSC.2015.7355993.